Ultrasonic Resonance Spectroscopy of Composite Rings for Flywheel Rotors

Laura M. Harmon
Cleveland State University, Cleveland, Ohio

George Y. Baaklini
Glenn Research Center, Cleveland, Ohio

The NASA STI Program Office . . . in Profile

Since its founding, NASA has been dedicated to the advancement of aeronautics and space science. The NASA Scientific and Technical Information (STI) Program Office plays a key part in helping NASA maintain this important role.

The NASA STI Program Office is operated by Langley Research Center, the Lead Center for NASA's scientific and technical information. The NASA STI Program Office provides access to the NASA STI Database, the largest collection of aeronautical and space science STI in the world. The Program Office is also NASA's institutional mechanism for disseminating the results of its research and development activities. These results are published by NASA in the NASA STI Report Series, which includes the following report types:

- TECHNICAL PUBLICATION. Reports of completed research or a major significant phase of research that present the results of NASA programs and include extensive data or theoretical analysis. Includes compilations of significant scientific and technical data and information deemed to be of continuing reference value. NASA's counterpart of peer-reviewed formal professional papers but has less stringent limitations on manuscript length and extent of graphic presentations.

- TECHNICAL MEMORANDUM. Scientific and technical findings that are preliminary or of specialized interest, e.g., quick release reports, working papers, and bibliographies that contain minimal annotation. Does not contain extensive analysis.

- CONTRACTOR REPORT. Scientific and technical findings by NASA-sponsored contractors and grantees.

- CONFERENCE PUBLICATION. Collected papers from scientific and technical conferences, symposia, seminars, or other meetings sponsored or cosponsored by NASA.

- SPECIAL PUBLICATION. Scientific, technical, or historical information from NASA programs, projects, and missions, often concerned with subjects having substantial public interest.

- TECHNICAL TRANSLATION. English-language translations of foreign scientific and technical material pertinent to NASA's mission.

Specialized services that complement the STI Program Office's diverse offerings include creating custom thesauri, building customized data bases, organizing and publishing research results . . . even providing videos.

For more information about the NASA STI Program Office, see the following:

- Access the NASA STI Program Home Page at *http://www.sti.nasa.gov*

- E-mail your question via the Internet to help@sti.nasa.gov

- Fax your question to the NASA Access Help Desk at 301–621–0134

- Telephone the NASA Access Help Desk at 301–621–0390

- Write to:
  NASA Access Help Desk
  NASA Center for AeroSpace Information
  7121 Standard Drive
  Hanover, MD 21076

Ultrasonic Resonance Spectroscopy of Composite Rings for Flywheel Rotors

Laura M. Harmon
Cleveland State University, Cleveland, Ohio

George Y. Baaklini
Glenn Research Center, Cleveland, Ohio

National Aeronautics and
Space Administration

Glenn Research Center

November 2001

ULTRASONIC RESONANCE SPECTROSCOPY OF COMPOSITE RINGS FOR FLYWHEEL ROTORS

Laura M. Harmon
Cleveland State University
Cleveland, Ohio 44115

George Y. Baaklini
National Aeronautics and Space Administration
Glenn Research Center
Cleveland, Ohio 44135

SUMMARY

Flywheel energy storage devices comprising multilayered composite rotor systems are being studied extensively for utilization in the International Space Station. These composite material systems were investigated with a recently developed ultrasonic resonance spectroscopy technique. The system employs a swept frequency approach and performs a fast Fourier transform on the frequency spectrum of the response signal. In addition, the system allows for equalization of the frequency spectrum, providing all frequencies with equal amounts of energy to excite higher order resonant harmonics. Interpretation of the second fast Fourier transform, along with equalization of the frequency spectrum, offers greater assurance in acquiring and analyzing the fundamental frequency, or spectrum resonance spacing. The range of frequencies swept in a pitch-catch mode was varied up to 8 MHz, depending on the material and geometry of the component. Single and multilayered material samples, with and without known defects, were evaluated to determine how the constituents of a composite material system affect the resonant frequency.

Amplitude and frequency changes in the spectrum and spectrum resonance spacing domains were examined from ultrasonic responses of a flat composite coupon, thin composite rings, and thick composite rings. Also, the ultrasonic spectroscopy responses from areas with an intentional delamination and a foreign material insert, similar to defects that may occur during manufacturing malfunctions, were compared with those from defect-free areas in thin composite rings. A thick composite ring with varying thickness was tested to investigate the full-thickness resonant frequency and any possible bulk interfacial bond issues. Finally, the effect on the frequency response of naturally occurring single and clustered voids in a composite ring was established.

INTRODUCTION

Flywheel energy storage devices comprising multilayered composite rotor systems are being studied extensively for use in the International Space Station (ISS). A flywheel system includes the components necessary to store and discharge energy in a rotating mass. The rotor is the complete rotating assembly portion of the flywheel primarily composed of a metallic hub and a composite rim as shown in figure 1. A shaft connects the hub to the rest of the flywheel system. The composite rim is the main rotating mass of the rotor responsible for generating and storing energy. The rim, as illustrated in figure 1, may contain several concentric composite rings, which include varying composite materials and geometries. This study investigated composite rings as candidates for composite rims in flywheel systems for the ISS. Each specimen consisted of a carbon-fiber-reinforced composite, a glass-fiber-reinforced composite, or varying combinations of these composite materials. The flat coupon was manufactured to mimic the manufacturing of the composite rings. These composite material systems were investigated with ultrasonic resonance spectroscopy (URS).

Ultrasonic spectroscopy is typically used in the nondestructive evaluation (NDE) of materials. Previously, ultrasonic spectroscopy demonstrated effectiveness in evaluating attenuation, velocity, and degradation in composite materials and ceramics; detecting and classifying discrete flaws, cracks, and corrosion; characterizing delaminations in composites; and analyzing multiple layered structures, adhesively bonded joints, and bonds between layers (refs. 1 to 7).
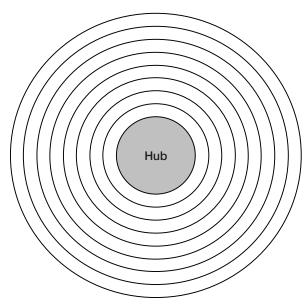
Figure 1.—Schematic of rotor illustrating a metallic
hub with a rim consisting of eight concentric rings.

A new resonance approach to ultrasonic spectroscopy was developed and patented (refs. 8 and 9). The system, UltraSpec (Southern Research Institute, Birmingham, AL), utilizes a continuous swept-frequency waveform, in a pitch-catch or through-transmission mode, with a direct contact setup. This technique requires performing an additional fast Fourier transform (FFT) on the frequency spectrum to find the fundamental resonant frequencies, or spectrum resonance spacing. The method's practical applications, to date, have shown more advances in detecting hidden corrosion in aluminum plates (ref. 8) and in evaluating bond quality in multiple layered structures (ref. 9) than previous ultrasonic spectroscopy methods have.

This approach should not be confused with Migliori's (ref. 10) swept sine approach to ultrasonic spectroscopy—resonant ultrasound spectroscopy—which excites full-specimen resonant vibration modes. This technique was developed to find the elastic moduli of specimens approximately 0.001 cm^3 in size.

This study examined the aforementioned URS as an NDE tool for quality assurance of composite rotor material systems in flywheel energy storage applications. A flat coupon and thin and thick composite rings from a composite concentric rim were investigated. The objectives were to determine (1) the effects of the constituents of single and multilayered composite material systems, and interfacial bond properties within those systems on the frequency responses and (2) the effects of intentionally seeded and naturally occurring flaws on the resonant frequencies in the various structures in order to assess the potential of URS as an NDE technique for certifying composite flywheels in the ISS.

Amplitude and frequency changes in the spectrum and spectrum resonance spacing domains were evaluated from the ultrasonic responses of a flat composite coupon, thin composite rings, and thick composite rings. The responses from areas with an intentional delamination and a foreign material insert, similar to defects that may occur during manufacturing, were compared with those from defect-free areas in thin composite rings. A thick composite ring with varying thickness was analyzed to investigate the full-thickness resonance. Finally, the effect of naturally occurring single and clustered voids in a thick composite ring on the resonance was established.

BACKGROUND

Previous Approaches to Ultrasonic Spectroscopy

Traditionally, a narrow ultrasonic signal was pulsed into a specimen with a piezoelectric broadband transducer creating a wide-bandwidth frequency response. Pulse-echo, pitch-catch, or through-transmission techniques were employed with direct contact or immersion modes. After ultrasound traveled through the specimen, a broadband transducer received the ultrasonic response in the time domain. A spectrum analyzer converted the ultrasonic pulse from the time domain to the frequency domain via Fourier transforms. The resulting spectrum was analyzed for amplitude and frequency changes. Fitting and Adler (ref. 2) produced an extensive review of the traditional methods of ultrasonic spectroscopy and their applications, which the reader should consult for more details.

Resonance Approach to Ultrasonic Spectroscopy

For the resonance approach to ultrasonic spectroscopy, an ultrasonic response in the time domain is converted to the frequency domain via Fourier transform. The resonance peak or peaks appearing in the frequency spectrum

represent higher order resonance peaks or harmonics. Since the value of each harmonic is a multiple of the fundamental frequency, the distance or spacing between each resonance is the fundamental frequency. The fundamental frequency results from a localized ultrasonic standing wave traveling through a specimen where the thickness is equal to half the wavelength. In the resonance approach to ultrasonic spectroscopy, the fundamental resonant frequency or spectrum resonance spacing is analyzed for changes in amplitude and frequency.

Resonance

The fundamental resonant frequency can be determined from an equation relating frequency to the thickness of a plate and the acoustic velocity in the plate. The fundamental relationship between the frequency f, wavelength λ, and acoustic velocity c, is

$$c = f\lambda \tag{1}$$

Rearranging these terms yields

$$f = \frac{c}{\lambda} \tag{2a}$$

At the fundamental resonant frequency f_R, there is a half wavelength in the plate thickness and

$$d = \frac{\lambda}{2} \tag{2b}$$

Solving for the wavelength λ yields

$$\lambda = 2d \tag{3}$$

Substituting equation (3) into equation (2) yields

$$f_R = \frac{c}{2d} \tag{4}$$

Rearranging the terms and solving for d yields

$$d = \frac{c}{2f_R} \tag{5}$$

Ultrasonic Resonance Spectroscopy

The ultrasonic spectroscopy system employed in the analysis was UltraSpec, which includes a digital processing oscilloscope, amplifier, digital-to-analog converter, and necessary computer software. The computer programs generate a continuous swept-frequency acoustic wave and capture the frequency response of a test specimen. The frequency sweep or interval is user defined with capabilities from the audible range to 8 MHz (Tucker, James: Re: Rules of Thumb. Personal communication. July 29, 1999). Figure 2 depicts the URS process with the ultrasonic spectroscopy system. The computer program generates a digital input waveform, shown in figure 2(a). The digital input waveform is then converted to an analog signal and transmitted into the test specimen with a medium-damped direct contact transducer, illustrated in figure 2(b). The medium-damped transducer maintains a high level of energy while providing a spectrum with a wide bandwidth. After the ultrasound travels through the specimen, another medium-damped transducer receives the ultrasonic response, displayed in the time domain in figure 2(c). A digital spectrum analyzer converts the ultrasonic wave from the time domain to the frequency domain via FFT, shown in figure 2(d). The resonant frequency peaks appearing in the spectrum contain the fundamental resonance or harmonics as exhibited by the material system under investigation. Since the value of each harmonic is an integer multiple
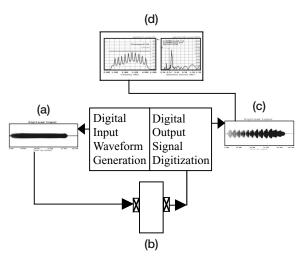
Figure 2.—Through-transmission ultrasonic spec-
troscopy on a Lucite sample. (a) Digital input
waveform in the time domain. (b) Ultrasonic spec-
troscopy system. (c) Digital output waveform in
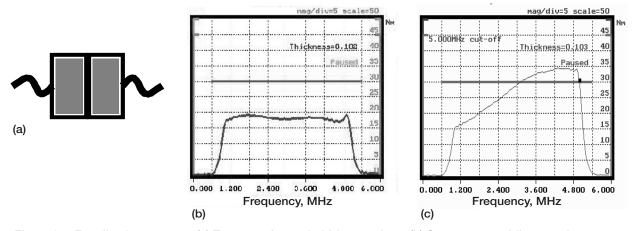the time domain. (d) Typical output display.

Figure 3.—Equalization process. (a) Two transducers held face-to-face. (b) Spectrum providing equal amounts
of energy to each frequency. (c) Spectrum providing larger amounts of energy to higher frequencies.

of the fundamental frequency, the spacing between each resonance represents the fundamental frequency. Conse-
quently, when a second FFT is performed on the spectrum, it produces the spectrum resonance spacing, or the fun-
damental resonant frequency.

To eliminate the effects of a nonlinear transducer response, the system has the capability of equalizing the
amount of energy distributed to each frequency. Equalization is accomplished by coupling the transducers face-
to-face, as illustrated in figure 3(a). An example of the resulting input spectrum after equalization is shown in
figure 3(b). When highly attenuating materials are being evaluated, more energy at higher frequencies is desirable,
as was the case in the present study. To compensate for energy lost due to attenuation, one should devote more
energy to the higher frequencies. This results in a frequency spectrum such as the one depicted in figure 3(c).

SPECIMENS AND EXPERIMENTAL PROCEDURES

Specimens

Ultrasonic spectroscopy measurements were taken along the circumference of five thin composite rings and two thick composite rings from a composite rim. Three of the thin composite rings (HB1.2.1, HB1.3.1, and HB1.4.5) consisted of one layer of carbon-fiber-reinforced epoxy matrix composite. HB1.2.1 was manufactured without intentionally seeded flaws. HB1.3.1 had one intentional flaw, a foreign material insert, built in. HB1.4.5 was delaminated intentionally at the midplane from 0° to 180°. The remaining two thin composite rings, HB1.7.13 and HB1.7.14, consisted of three composite layers. One layer of glass-fiber-reinforced composite was sandwiched between two layers of carbon-fiber-reinforced composite. Both rings were manufactured without intentional flaws. The flat sample, FP4–1A, consisted of three composite layers equivalent to the structures of HB1.7.13 and HB1.7.14.

The structures of the thick composite rings, log drop 1.4 and R2.6, were very similar to one another. URS evaluation performed on log drop 1.4 investigated changes in resonant frequencies due to the thinning of various sections. Sections were milled from the ring in a stepwise function, as shown in figure 4. A thick section was milled from region (e) of the ring. Thinner sections were milled from regions (d), (c), and (b). Region (a) remained intact. URS evaluation was done before and after removing these sections. The R2.6 ring exhibited regions affected by manufacturing flaws. One region of R2.6 had a single void, shown in figure 5(b), 1 mm (0.03 in.) into the ring. Another region had a cluster of small voids, shown in figure 5(c), 7.7 mm (0.3 in) into the ring. The remainder of R2.6 was defect free.
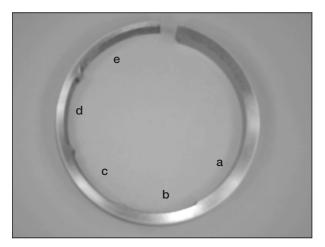

Figure 4.—Log drop 1.4 with composite sections removed, where region (a) remained intact, (b) had one section removed, and (c), (d), and (e) had increasingly thicker sections removed.
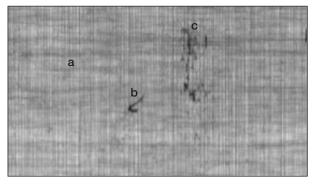

Figure 5.—Ultrasonic C-scan image of a section of R2.6 showing the presence of (a) an unflawed region, (b) a void 1.0 mm into the ring, and (c) a void cluster 7.7 mm into the ring.

Experimental Procedures

All specimens were evaluated in the pitch-catch mode of ultrasonic transmission with direct contact. The transducers were coupled to the outer diameter of the rings with Panametrics couplant A (propylene glycol) or couplant D (gel). Coaxial cables connected the transducers to the transmitter and receiver. Medium-damped transducers were employed to maximize energy while keeping the bandwidth broad. The transducer frequency was dependent on the upper limit of the frequency sweep. Ultran WC50 medium-damped transducers (5 and 10 MHz) maximized energy while keeping the bandwidth broad (Tucker, James: Personal communication. April 10, 2000).

RESULTS AND ANALYSIS

Acoustic Velocities

The out-of-plane (i.e., through-the-thickness) acoustic velocities of the carbon-fiber-reinforced composite and the glass-fiber-reinforced composite employed for analysis of the three-layer composite ring systems (HB1.7.13 and HB1.7.14), the three-layer composite flat coupon system (FP4–1A), and the thick composite rings (log drop 1.4 and R2.6) were derived from resonances resulting from URS and equation (4). For the carbon-fiber-reinforced composite, the acoustic velocity resulted from the unflawed regions of HB1.2.1, HB1.3.1, and HB1.4.5. The acoustic velocities from approximately 70 locations were averaged for the carbon-fiber-reinforced composite as 2.97 mm/μsec (0.117 in./μsec). For the glass-fiber-reinforced composite, the acoustic velocity came from the average of 10 resonance measurements on a sample of glass-fiber-reinforced composite as 3.81 mm/μsec (0.150 in./μsec).

These acoustic velocities were verified with acousto-ultrasonics or time-of-flight measurements as 3.12 mm/μsec (0.123 in./μsec) for the carbon-fiber-reinforced composite and 3.74 mm/μsec (0.147 in./μsec) for the glass-fiber-reinforced composite. Both acoustic velocities were within 5 percent of the acoustic velocities derived from URS. Since the acoustic velocities of the two composites were different, the acoustic velocity of each specimen was calculated as a weighted average by volume from the constituents of the specimen. The percentage by volume of each composite present at a specified depth was multiplied by the respective acoustic velocities as follows

$$c_{TL} = x_c c_c + x_g c_g \tag{6}$$

where c_{TL} was the weighted average by volume of the acoustic velocity up to a particular lamina in the specimen, x_c and x_g were the percentages by volume of the carbon-fiber-reinforced composite and the glass-fiber-reinforced composite, and c_c and c_g were the acoustic velocities of the carbon-fiber-reinforced composite and the glass-fiber-reinforced composite. Hence, c_c and c_g can be calculated when x_c and x_g differ on two regions of a given specimen.

One-Layer Composite Ring (HB1.2.1)

Figure 6 shows the typical ultrasonic response produced by a one-layer composite ring manufactured without flaws. The information presented shows a typical spectrum and spectrum resonance spacing created by pulsing a 1- to 5-MHz frequency sweep in the pitch-catch mode through an undamaged composite lamina. The spectrum shows six peaks representing the frequency content present between 1 and 5 MHz. The spectrum resonance spacing domain shows a sharp peak at 0.620±0.008 MHz representing the resonance for the full thickness of 2.421 mm (0.0953 in.). A sharp peak indicates a high impedance mismatch. In this particular case, it would be the impedance mismatch between the composite and air. Also note the smaller peak in the spectrum resonance spacing domain. This peak occurs at 0.310 MHz, which is exactly half the fundamental resonant frequency, 0.620 MHz. This reso-
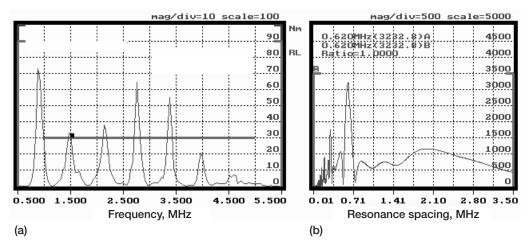

Figure 6.—Ultrasonic response for HB1.2.1. (a) Spectrum plot. (b) Spectrum resonance spacing plot.

nant frequency is an example of a frequency resulting from the quarter wavelength in the specimen. In addition, broad humps of low amplitude followed the sharp peak. They were of high frequency and did not add any substantial explanation to understanding sound propagation in the ring.

One-Layer Composite Ring With Foreign Material Insert (HB1.3.1)

Figure 7 shows the region of ring HB1.3.1 with the foreign material insert. Figure 8 presents plots of the spectrum and spectrum resonance spacing domains for locations with and without the foreign material insert. In a portion of the ring without the insert, the fundamental resonant frequency for the full thickness of 2.527 mm (0.0995 in.)

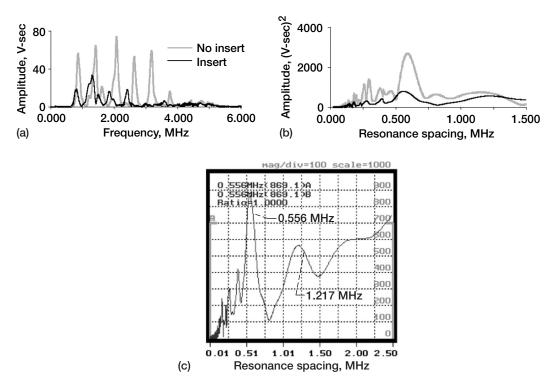Figure 7.—Optical photograph of HB1.3.1 at the insert.

Figure 8.—Data for HB1.3.1 at the location with and without the insert. (a) Spectrum plot. (b) Spectrum resonance spacing plot. (c) Spectrum resonance spacing at the location with the insert on a smaller scale.

appeared as a single major peak at 0.584±0.008 MHz in the spectrum resonance spacing domain. Neglecting the presence of the insert, the fundamental resonant frequency was calculated to be 0.544 MHz for a thickness of 2.73 mm (0.1075 in.). The actual resonant frequency at the location with the insert was 0.556±0.008 MHz, as shown in figure 8(c). The obvious differences between the ultrasonic response for the region with and without the insert were the reduction in amplitude and the change in resonant frequency. The resonant frequency may be larger than the calculated resonant frequency because of a higher velocity in the material inserted into HB1.3.1. Overall amplitudes of both the spectrum and spectrum resonance spacing decreased by at least half in comparison to the response for the location without an insert because of scattering of the signal at the insert. Furthermore, fewer frequencies were excited in the spectrum. A broad hump also existed at 1.217±0.008 MHz, shown on a smaller scale in figure 8(c). The frequency detected at 1.217 MHz may correspond to the resonance of the outer carbon composite layer. The resonant frequency for the layer between the insert and the outer diameter may not be fully resolved because (1) only a few frequencies were excited in the spectrum or (2) the interface was not degraded enough to cause a sizeable resonance peak.

One-Layer Composite Ring With Intentional Delamination (HB1.4.5)

Figure 9 illustrates a delamination, which appears to be rather smooth. The ultrasonic response for this region is compared with the ultrasonic response for a region without a delamination in figure 10. A resonant frequency peak at 1.151±0.008 MHz, corresponding to a thickness of 1.290 mm (0.0508 in.) appeared in the spectrum resonance spacing domain for the location with the delamination. The actual distance from the outer diameter to the location of the delamination was 1.311 mm (0.0516 in.). Therefore, the location of the delamination was determined within a 2-percent error in comparison to optics from the resonant frequency response. The full-thickness resonance did not appear. Another observation was the peak splitting that occurred in the spectrum domain, which did not occur with the undamaged region of HB1.4.5. Two smaller resonances at 0.372±0.008 and 0.564±0.008 MHz in the resonance
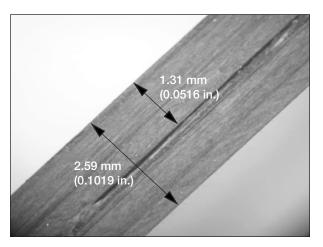

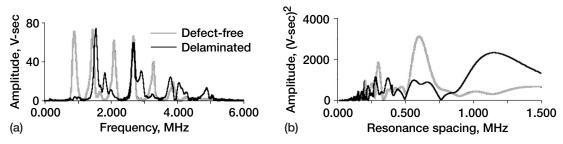Figure 9.—Optical photograph of the delamination at the midplane of HB1.4.5.

Figure 10.—Measurements at delaminated and defect-free regions of HB1.4.5. (a) Spectrum plot. (b) Spectrum resonance spacing plot.

spacing domain may have resulted from the peak splitting. In comparison to the undelaminated region, the amplitude of the spectrum resonance spacing domain decreased. This decrease in amplitude was indicative of absorbed or scattered energy due to the delamination.

Figure 11 exhibits a delaminated region of a different structure than the delamination in figure 9. The ultrasonic response for this delaminated region is compared with a defect-free region in figure 12. The ultrasonic response for the delaminated region detected resonant frequency peaks at 1.127±0.008 and 0.573±0.008 MHz. The resonance at 0.573 MHz corresponds to the full thickness, whereas the resonance at 1.127 MHz corresponds to 1.31 mm (0.052 in.) from the outer diameter. The actual location of 1.28 mm (0.051 in.) is shown in figure 11. Hence, the location of the delamination was determined within a 2.5-percent error in comparison to optics from the frequency
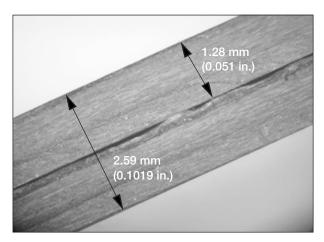

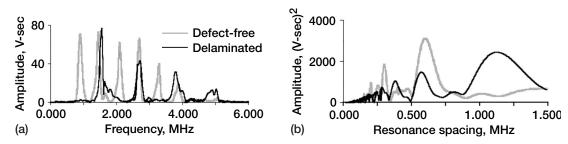Figure 11.—Optical photograph of the delamination in HB1.4.5.

Figure 12.—Ultrasonic response for HB1.4.5 at the location shown in figure 11 and a defect-free region. (a) Spectrum plot. (b) Spectrum resonance spacing plot.

results provided by URS. The amplitude of the full-thickness resonant frequency was approximately two-thirds that of the resonant frequency for the thickness to the delamination, indicating that more energy returned from the delamination than from the full thickness. Comparing the optical photos of the delaminated regions in figures 9 and 11 and their responses illustrates that different types of delaminations produce different ultrasonic responses.

Three-Layer Composite Ring System (HB1.7.13 and HB1.7.14)

The ultrasonic responses for two three-layer composite ring systems, HB1.7.13 and HB1.7.14, are shown in figure 13. The full-thickness resonance appeared at 0.610±0.008 and 0.586±0.008 MHz for HB 1.7.13 and HB1.7.14, respectively.

A comparison of the ultrasonic response for a one-layer composite ring to the responses for the three-layer composite rings, shown in figure 13, illustrates similarities between the responses. The amplitude of the resonant frequency for the ring with three composite layers (fig. 13) is approximately the same as that for the systems with one composite layer. Another observation is the appearance of a major peak in the spectrum resonance spacing domains
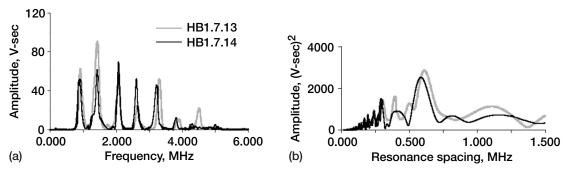
Figure 13.—Data for two defect-free three-layer composite rings. (a) Spectrum plot. (b) Spectrum resonance spacing plot.

indicating the fundamental resonant frequency for the full thickness. Therefore, in a well-bonded three-layer composite ring, the full thickness resonated, just as it did for the one-layer composite ring.

Three-Layer Composite Flat Coupon System (FP4-1A)

Consisting of three layers of composite material, the flat coupon, FP4-1A, was manufactured to mimic the manufacturing of the rings. Figure 14 compares the responses for the three-layer composite flat coupon and a three-layer composite ring. The value of the peak in the spectrum resonance spacing domain was 0.792±0.008 MHz, as shown in figure 14(c). The calculated fundamental resonant frequency of 0.865 MHz for the thickness of 1.725 mm (0.0679 in.) does not fall within the allowable error of the result produced with URS. Peaks corresponding to individual layers or combinations of layers did not appear. This does not necessarily mean that the flat coupon was well bonded throughout. Only one harmonic appeared in the frequency spectrum, so the resonances corresponding to the individual layers could not be resolved.
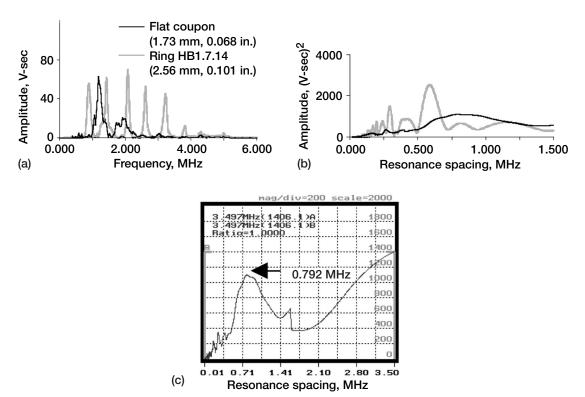

Figure 14.—Ultrasonic data for the flat coupon and the three-layer composite ring. (a) Spectrum plot. (b) Spectrum resonance spacing plot. (c) Spectrum resonance spacing for the flat coupon on a smaller scale.

A comparison to the responses from the three-layer composite rings aids in the explanation of the ultrasonic spectroscopy response from the flat coupon, shown in figure 14. The structure of the resonant frequency peak in the spectrum resonance spacing domain was completely different from that produced by the three-layer composite rings. The resonant frequency peak for FP4–1A was not sharp, whereas the resonant frequency peaks for the three-layer composite rings were sharp. In addition, very few resonant frequencies were excited for FP4–1A in the spectrum domain, figure 14(a). The lack of resonant frequencies in the spectrum results in the dull peak in the spectrum reso- nance spacing. Not enough frequencies were excited to resolve a sharp peak. Finally, the amplitude of the resonant frequency peak was less than half that produced for the three-layer composite ring.

Results indicated that manufacturing of the flat coupon did not duplicate the properties of the rings, as the ultra- sonic signal scattered enough to prevent many resonant frequencies from being excited in the frequency spectrum. The resulting resonant frequency peak was broad and of low amplitude. Also, the fundamental resonant frequency differed from the calculated resonance. The manufacturing process produced different anomalies, such as fiber bunching. Hence, caution should be exercised if these coupons are to be used in material characterization, since they may not truly mimic the material utilized for the flywheels.

Log Drop 1.4

Figure 15 illustrates the response for section (c) in figure 4 at a thickness of 7.72 mm (0.3041 in.). Only the resonant frequency for the full thickness is present at 0.205 MHz in the spectrum resonance spacing. This response is typical of the ultrasonic responses for each section of the ring. Resonant frequencies corresponding to locations within the thickness were not present in the spectrum resonance spacing domain, meaning the full thickness reso- nated as one system and the system was well bonded. In an unaltered section of log drop 1.4, shown in figure 4(a), the spectrum resonance spacing window illustrated one full-thickness resonance peak at 0.142±0.008 MHz, just as it did for region (c). The full-thickness resonance of 0.146 MHz was calculated using the weighted average for the velocity. This fundamental resonant frequency of 0.146 MHz fell within the error of the resonance peak at 0.142±0.008 MHz.

As expected, when the thickness decreased, the resonant frequency increased. The thicknesses, estimated reso- nant frequencies for those thicknesses, and resonant frequency peaks observed with the ultrasonic spectroscopy sys- tem at each region of the machined log drop 1.4 are listed in table I. The resulting resonant frequencies at each location before and after thinning sections are shown visually in figure 16.
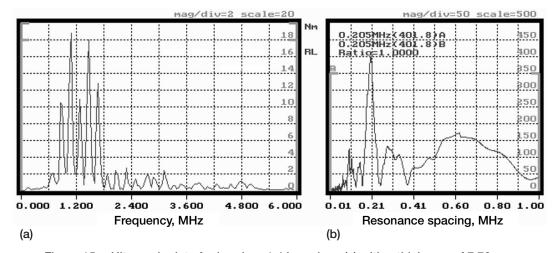

Figure 15.—Ultrasonic data for log drop 1.4 in regions (c) with a thickness of 7.72 mm (0.3041 in.). (a) Spectrum plot. (b) Spectrum resonance spacing plot.

TABLE I.—RESONANT FREQUENCIES FOR LOG DROP 1.4

Section	(a)	(b)	(c)	(d)	(e)
Full thickness, mm (in.)	10.87	9.14	7.72	6.30	4.94
	(.4280)	(.3598)	(.3041)	(.2481)	(.1943)
Calculated resonant frequency,[a] MHz	.146	.174	.206	.255	.333
URS resonant frequency, MHz	.142	.171	.205	.245	.311

[a]See the acoustic velocities section for description of calculated resonant frequencies.
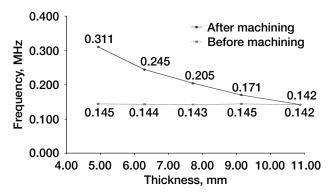
Figure 16.—Resonance from different sections of log drop 1.4 before and after machining.

R2.6

Three locations of interest for R2.6 are shown in figure 5: a defect-free region (a), a void 1 mm (0.04 in.) into the ring (b), and a void cluster 7.7 mm (0.3 in.) into the ring (c).

Figure 17 compares responses from the defect-free region and the region with the void 1 mm (0.04 in.) from the outer diameter. For the defect-free region, one sharp peak was present at 0.118±0.008 MHz, representing the full-thickness resonance. In addition to the full-thickness resonance, a sharp peak at 0.157±0.008 MHz appeared, representing an approximate thickness of 9.6 mm (0.38 in.) from the outer diameter of the ring. Both peaks appeared in all regions of R2.6, flawed and unflawed. The existence of such a sharp peak may be indicative of a kissing disbond approximately 9.6 mm (0.38 in.) into R2.6. Results need to be further investigated to corroborate the existence of a kissing disbond. Less defined peaks at 0.248, 0.312, and 0.494 MHz, corresponding to approximate thicknesses of 6.1 mm (0.24 in.), 5.5 mm (0.22 in.), and 4 mm (0.16 in.) from the outer diameter emerged in the response for the defect-free region. Further NDE is necessary to verify the source of the resonance peaks because computed tomography did not locate defects at these locations (see figs. 18 and 19). The void in figure 5(b), with a 4.1-mm (0.16-in.) width perpendicular to the ultrasonic wave path, produced the ultrasonic response also shown in figure 17. The calculated fundamental resonant frequency for the location of the void, shown in figure 18, 1.0 mm (0.04 in.) into the ring, was 1.875 MHz. This frequency was not resolved in the spectrum resonance spacing window because the spectrum domain only excited the fundamental frequency. No additional harmonics appeared in the spectrum. For a resonance to be resolved in the spectrum resonance spacing domain, at least two peaks are necessary in the spectrum domain. Because of time constraints, another wider sweep was not performed. However, there were observable changes in the ultrasonic spectroscopy response for the region without the void. The amplitude of the full-thickness
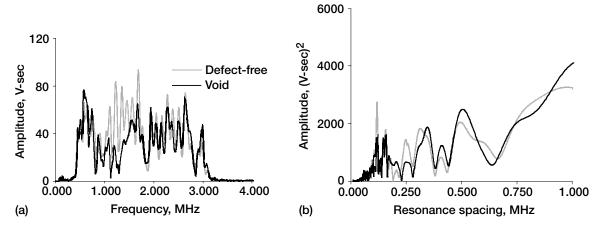

Figure 17.—Ultrasonic data for regions with and without the void 1.0 mm into R2.6. (a) Spectrum plot. (b) Spectrum resonance spacing plot.
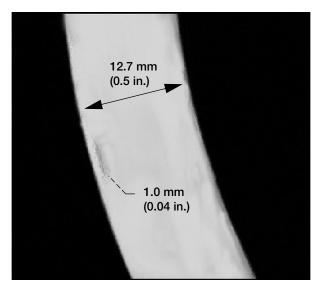
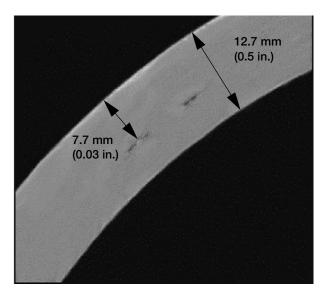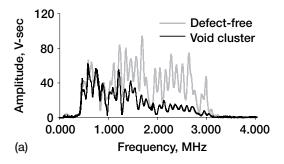Figure 18.—Computed tomography image showing location of void in R2.6.

Figure 19.—Computed tomography image illustrating the location of the void cluster in R2.6.
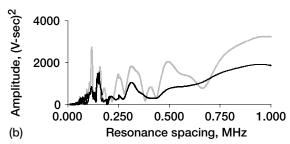

(a)

(b)

Figure 20.—Ultrasonic responses for the defect-free region and the region with the void cluster 7.7 mm (0.3 in.) into R2.6. (a) Spectrum plot. (b) Spectrum resonance spacing plot.

resonance, at roughly 0.118 MHz, decreased by approximately 40 percent. Less energy returned through the full thickness. The resonant frequency at 0.147 MHz represents a shift outside the error of the 0.157-MHz peak, but it remained at the same amplitude. The peaks at 0.248 and 0.312 MHz completely disappeared from the resonance spacing window with a new peak at 0.346 MHz taking their place. The new peak corresponds to a thickness 5.0 mm (0.20 in.) into the ring. The amplitude of a peak at approximately 0.494 MHz increased.

Figure 20 compares responses for a defect-free region and the region with the void cluster. For the void cluster region spanning 12.2 mm (0.48 in.) perpendicular to the ultrasonic wave path, shown in figures 5(c) and 20, at a location of 7.7 mm (0.3 in.) into the ring, the calculated fundamental resonance frequency was 0.210 MHz. This peak did not appear in the response in figure 19, although the overall amplitude decreased. The only three peaks that remained in comparison to the unflawed region were 0.118, 0.157, and 0.312 MHz. The amplitude of the full-thickness resonance reduced by approximately 60 percent. In addition, the frequency spectrum indicated significant changes in amplitude, especially for the frequencies beyond 1.800 MHz. The frequencies beyond 1.800 MHz also decreased by approximately 60 percent.

Comparing the ultrasonic response from the defect-free region to the response from the region with the void, the amplitudes of the full-thickness resonance decreased by approximately 40 percent with an overall reduction in the frequency spectrum. A resonance corresponding to the location of the void, 1.0 mm (0.04 in.) from the outer diameter of ring R2.6, was not resolved in the spectrum resonance spacing. In comparison to the defect-free region to the region with the void cluster, the amplitude of the full-thickness resonance and the spectrum above 1.800 MHz decreased by approximately 60 percent. A resonance corresponding to the location of the void cluster did not appear. Therefore, the URS evaluation detected the presence of damage with a reduction in amplitude only.

SUMMARY OF FINDINGS

URS evaluation of thin composite rings yielded a number of results. A defect-free one-layer composite ring produced the full-thickness fundamental resonant frequency. The presence and location of a delamination, within a single layer of composite material, were determined from the change in resonant frequency. Delaminations of different structures produced response signals with different features. The presence of a foreign material insert in a single-layer composite ring reduced the amplitude in the spectrum and spectrum resonance spacing. In addition, the value of the resonant frequency changed because of the increased thickness of the section and due to the difference in the acoustic velocity of the inserted material. A defect-free three-layer composite ring system produced the full-thickness resonance, indicating good bonding at the interfaces. However, URS results for the three-layer composite flat coupon exhibited major changes in the spectrum and resonant frequency. These changes indicated that the manufacturing of the flat coupon did not mimic that of the rings.

Well-bonded composite thick rings resonated the full thickness only, with a single sharp resonant frequency in the spectrum resonance spacing domain. In addition, full-thickness resonances increased in value as the thickness decreased in different sections of the composite ring.

Data from naturally occurring single and clustered voids in a thick composite ring indicated that a single 4.1-mm- (0.16-in.-) wide and 0.8-mm- (0.03-in.-) thick void, 1.0 mm below the surface, caused a 40-percent reduction in the full-thickness resonance in the spectrum resonance spacing domain and a general decrease in the spectrum domain. Clustered voids 7.7 mm below the surface reduced the amplitudes of the full-thickness resonance in the spectrum resonance spacing domain by 60 percent. Frequencies above 1.8 MHz in the spectrum domain were reduced by 60 percent. However, the locations of the single void and the void cluster were not detected. In addition, ultrasonic data detected possible kissing disbonds, which were undetected by other NDE methods.

CONCLUSIONS

Ultrasonic resonance spectroscopy (URS) was employed to investigate composite rings for use in a flywheel rotor system. Amplitude and frequency changes in the spectrum and spectrum resonance spacing domains were evaluated to establish the foundation for characterizing the damage state in the composite rings targeted for flywheel technology insertion in the International Space Station.

This study established URS as a potential nondestructive evaluation (NDE) method for flywheel composite rotor evaluation. The full-thickness resonance was produced in defect-free thick and thin composite rings. The presence of foreign materials and delaminations in composite rings was detected as an amplitude reduction in the spectrum domain and change in resonant frequency in the spectrum resonance spacing domain. URS discerned between the manufacturing of a flat composite coupon and composite rings, since major differences between ultrasonic response signals were detected. The presence of naturally occurring discrete and clustered voids, with a width greater than 4.1 mm (0.16 in.) perpendicular to the ultrasonic wave path, was detected in a multilayered thick ring with an amplitude reduction in the spectrum and spectrum resonance spacing. The unique detection of kissing disbonds by URS requires further investigation, as their existence in the multilayered composite ring was not confirmed destructively through metallographic sectioning, or corroborated with other nondestructive techniques. On the basis of these findings, URS is a potential NDE method for flight certification of composite rings to be used in the International Space Station. Future research will investigate URS for flight certification of composite rims.

REFERENCES

1. Birks, Albert S.; Green, Robert E.; and McIntire, Paul: Ultrasonic Testing. Second ed., American Society for Nondestructive Testing, Columbus, OH, 1991.
2. Fitting, Dale W.; and Adler, Laszlo: Ultrasonic Spectral Analysis for Nondestructive Evaluation. Plenum Press, New York, NY, 1981.
3. Sharpe, R.S.: Research Techniques in Nondestructive Testing. Academic Press, New York, NY, 1970.
4. Krautkrämer, Josef, et al.: Ultrasonic Testing of Materials. Second ed., Springer-Verlag, New York, NY, 1977.

5. Stiffler, Richard C.; Henneke, Edmund C., II; and Duke, J.C., Jr.: The Application of Ultrasonic Spectrum Analysis for Determining the Damage State in Advanced Composite Materials Undergoing Cyclic Loading. ASNT National Conference, Boston, MA, 1982, pp. 95–99.

6. Schueneman, G.T., et al.: Evaluation of Short Term—High Intensity Thermal Degradation of Graphite Fiber Reinforced Laminates via Ultrasonic Spectroscopy. J. Polym. Sci. Part B: Polym. Lett., vol. 37, 1999, pp. 2601–2610.

7. Kliger, Howard S., et al.: Materials and Process Affordability; Keys to the Future. Paper presented at the 43rd International SAMPE Symposium and Exhibition, Covina, CA, 1998.

8. Tucker, James R.: Ultrasonic Spectroscopy for Corrosion Detection and Multiple Layer Bond Inspection. Proceedings of the First Joint DoD/FAA/NASA Conference on Aging Aircraft, vol. II, 1998, pp. 1537–1550.

9. Chambers, J.K.; and Tucker, J.R.: Bondline Analysis Using Swept-Frequency Ultrasonic Spectroscopy. INSI, vol. 41, no. 3, 1999, pp. 151–155.

10. Migliori, A., et al.: Resonant Ultrasound Spectroscopic Techniques for Measurement of the Elastic Moduli of Solids. Physica B, vol. 183, 1993, pp. 1–24.

REPORT DOCUMENTATION PAGE

Public reporting burden for this collection of information is estimated to average 1 hour per response, including the time for reviewing instructions, searching existing data sources, gathering and maintaining the data needed, and completing and reviewing the collection of information. Send comments regarding this burden estimate or any other aspect of this collection of information, including suggestions for reducing this burden, to Washington Headquarters Services, Directorate for Information Operations and Reports, 1215 Jefferson Davis Highway, Suite 1204, Arlington, VA 22202-4302, and to the Office of Management and Budget, Paperwork Reduction Project (0704-0188), Washington, DC 20503.

1. AGENCY USE ONLY (*Leave blank*)	2. REPORT DATE	3. REPORT TYPE AND DATES COVERED
	November 2001	Technical Memorandum

4. TITLE AND SUBTITLE

Ultrasonic Resonance Spectroscopy of Composite Rings for Flywheel Rotors

6. AUTHOR(S)

Laura M. Harmon and George Y. Baaklini

5. FUNDING NUMBERS

WU–755–1A–09–00

7. PERFORMING ORGANIZATION NAME(S) AND ADDRESS(ES)

National Aeronautics and Space Administration
John H. Glenn Research Center at Lewis Field
Cleveland, Ohio 44135–3191

8. PERFORMING ORGANIZATION REPORT NUMBER

E–12816

9. SPONSORING/MONITORING AGENCY NAME(S) AND ADDRESS(ES)

National Aeronautics and Space Administration
Washington, DC 20546–0001

10. SPONSORING/MONITORING AGENCY REPORT NUMBER

NASA TM—2001-210960

11. SUPPLEMENTARY NOTES

Prepared for the Sixth Annual International Symposium on NDE for Health Monitoring and Diagnostics sponsored by The International Society for Optical Engineering, Newport Beach, California, March 4–8, 2001. Laura M. Harmon, Cleveland State University, 1983 East 24th Street, Cleveland, Ohio 44115–2403; and George Y. Baaklini, NASA Glenn Research Center. Responsible person, George Y. Baaklini, organization code 5920, 216–433–6016.

12a. DISTRIBUTION/AVAILABILITY STATEMENT

Unclassified - Unlimited
Subject Categories: 38 and 20   Distribution: Nonstandard

Available electronically at http://gltrs.grc.nasa.gov/GLTRS

This publication is available from the NASA Center for AeroSpace Information, 301–621–0390.

12b. DISTRIBUTION CODE

13. ABSTRACT *(Maximum 200 words)*

Flywheel energy storage devices comprising multilayered composite rotor systems are being studied extensively for utilization in the International Space Station. These composite material systems were investigated with a recently developed ultrasonic resonance spectroscopy technique. The system employs a swept frequency approach and performs a fast Fourier transform on the frequency spectrum of the response signal. In addition, the system allows for equalization of the frequency spectrum, providing all frequencies with equal amounts of energy to excite higher order resonant harmonics. Interpretation of the second fast Fourier transform, along with equalization of the frequency spectrum, offers greater assurance in acquiring and analyzing the fundamental frequency, or spectrum resonance spacing. The range of frequencies swept in a pitch-catch mode was varied up to 8 MHz, depending on the material and geometry of the component. Single and multilayered material samples, with and without known defects, were evaluated to determine how the constituents of a composite material system affect the resonant frequency. Amplitude and frequency changes in the spectrum and spectrum resonance spacing domains were examined from ultrasonic responses of a flat composite coupon, thin composite rings, and thick composite rings. Also, the ultrasonic spectroscopy responses from areas with an intentional delamination and a foreign material insert, similar to defects that may occur during manufacturing malfunctions, were compared with those from defect-free areas in thin composite rings. A thick composite ring with varying thickness was tested to investigate the full-thickness resonant frequency and any possible bulk interfacial bond issues. Finally, the effect on the frequency response of naturally occurring single and clustered voids in a composite ring was established.

14. SUBJECT TERMS

Ultrasonic spectroscopy; Spectrum analysis; Resonance; Resonant frequencies; Composite materials; Flywheels; Rotors; Nondestructive tests

15. NUMBER OF PAGES

21

16. PRICE CODE

17. SECURITY CLASSIFICATION OF REPORT	18. SECURITY CLASSIFICATION OF THIS PAGE	19. SECURITY CLASSIFICATION OF ABSTRACT	20. LIMITATION OF ABSTRACT
Unclassified	Unclassified	Unclassified	